

Atomic Dynamics in Strongly Coupled Multimode Cavities under Continuous Measurement

Valentin Link,¹ Kai Müller,¹ Rosaria G. Lena,² Kimmo Luoma,³ François Damanet,⁴ Walter T. Strunz,¹ and Andrew J. Daley²

¹*Institut für Theoretische Physik, Technische Universität Dresden, D-01062 Dresden, Germany.*

²*Department of Physics and SUPA, University of Strathclyde, G4 0NG Glasgow, United Kingdom.*

³*Department of Physics and Astronomy, University of Turku, FI-20014 Turun Yliopisto, Finland.*

⁴*Department of Physics and CESAM, University of Liège, B-4000 Liège, Belgium.*

(Dated: May 29, 2022)

Atoms in multimode cavity QED systems provide an exciting platform to study many-body phenomena in regimes where the atoms are strongly coupled amongst themselves and with the cavity. An important challenge in this, and other related non-Markovian open quantum systems is to understand what information we gain about the atoms from continuous measurement of the output light. In this work, we address this problem, describing the reduced atomic state via a conditioned hierarchy of equations of motion, which provides an exact conditioned reduced description under monitoring (and continuous feedback). We utilise this formalism to study how different monitoring for modes of a multimode cavity affects our information gain for an atomic state, and to improve spin squeezing via measurement and feedback in a strong coupling regime. This work opens opportunities to understand continuous monitoring of non-Markovian open quantum systems, both on a practical and fundamental level.

I. INTRODUCTION

In quantum mechanics, a continuous measurement intrinsically influences the dynamics of a system such that its state depends on the particular measurement record [1–9]. Theoretical techniques to describe this conditioned state of the system have been well established [10–12], and play a central role in quantum control theory. In particular, the measurement record can be used as a feedback signal to drive the system in a desired state [13, 14], counter decoherence [15] or increase entanglement [16, 17]. In recent years, interest has shifted from few particle systems to the control of many-body quantum systems. For example, there are opportunities to explore particularly interesting many-body physics [18–32] with many atoms in optical cavities in regimes where the atoms interact strongly amongst themselves and also with the cavity mode(s), as depicted in Fig. 1. In principle, we would like to understand what information we can infer about the state of the atoms from light leaking out of the cavity. However, especially in the case of multimode cavities [18–20, 23, 25–27], the problem becomes rapidly intractable as the system size and number of cavity modes grows.

In this work we present a new method to describe the information we obtain about the state of the atoms, which also contains a framework for understanding and utilising conditioned dynamics with continuous feedback. Our exact theory for the reduced state of the atoms (dashed blue box in Fig. 1) takes the form of a conditioned hierarchy of equations of motion, with the hierarchy capturing the information collectively present in the cavity mode(s). This theory thus accounts for a nontrivial interaction of the atoms with the cavity modes and vice versa, which makes the dynamics of the atoms non-

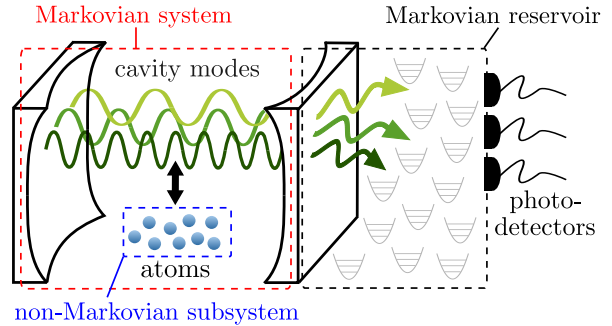


FIG. 1. Schematic setup, showing the gain of information about a many-body system of atoms in a multimode cavity, through detection of light leaking out of the cavity. While the combined cavity-atom system (red box) can be Markovian, it is a highly complex system with many modes. In the case of strong coupling between the atoms and the cavity, the reduced system of atoms (blue box) exhibits non-Markovian dynamics. Our formalism allows us to determine the information gained about this reduced system from the measurements, determining the measurement-conditioned dynamics, and allowing for continuous feedback.

Markovian. The efficiency of the hierarchical approach allows us to go beyond previous reduced descriptions for the state of the atoms in cases where the cavity modes can be adiabatically eliminated, addressing directly the strong coupling limit in a form that is also numerically tractable.

Although for concreteness we discuss the example of cavity QED, our theory can be applied to arbitrary quantum systems coupled to a non-Markovian bath which can be split into two parts with a larger Markovian open system in front of the detector. This includes networks of standard single-mode cavity QED, coupled resonator ar-

rays and circuit QED [33–35], systems of electrons coupled to damped phonons (i.e., a dissipative Hubbard-Holstein model [36]) relevant for the solid-state, systems of cold atoms immersed in a BEC [37] or coupled coherently to an untrapped level [38, 39], or quantum emitters coupled to plasmonic cavities [40] which can be modeled in terms of leaky quasinormal modes [41].

Furthermore, the formalism is itself an interesting extension to the general theory of open quantum systems. While established non-Markovian open system methods make it possible to compute the reduced state of the system (the atoms in Fig. 1) in the *unmonitored* case, making a connection to continuous measurement was possible only in some very special cases [42]. In contrast, here the exact non-Markovian dynamics of the atoms directly inherits a measurement interpretation from the full Markovian system of atoms and cavity modes. The embedding of a non-Markovian system in a larger Markovian system is a well known strategy [43–50]. However, our results provide a systematic exact theory to determine the *conditioned* states for the reduced system for different measurement schemes of the outgoing cavity field, connecting directly to various experimental setups.

Below in Section II, we introduce details on the cavity QED systems that we consider, and revise the corresponding continuous measurement theory. We also illustrate why in the strong coupling regime, standard adiabatic elimination of the cavity mode is not sufficient to accurately predict the dynamics of the atoms. In Section III, we present the derivation of our new exact description of the conditioned reduced atomic state, which takes the form of a conditioned hierarchy of mixed-state quantum trajectories for atom-only density matrices, inspired by other Hierarchical Equations of Motion (HEOM) methods [51, 52]. In Section IV, the application of our method to multimode cavities is discussed, and we study how the information we gain about the atomic system and the resulting correlations depend on the way in which the cavity modes are monitored. In Section V, we extend the theory to include quantum feedback based on the continuous measurement, which has direct applications in quantum control. We show how squeezing of a collective spin in cavity QED can be improved via feedback, beyond the results known in an adiabatic regime [13]. Finally, in Section VI, we present our conclusions and discuss further future perspectives arising from this work.

II. CONDITIONED ATOM DYNAMICS

While the physics that we address in this work is far more general, we will use the language of cavity QED. First, we choose as a concrete example a simple and well known model: a collection of atoms A , coupled to a single mode of an optical cavity C via the Hamiltonian

$$H_{AC} = H_A + \Delta a^\dagger a + g(aL^\dagger + a^\dagger L) \quad (1)$$

where H_A and L are respectively the Hamiltonian and an arbitrary coupling operator for the atoms, a is the cavity mode annihilation operator, and g is the atom-cavity mode coupling strength.

Multimode generalizations of this model constitute good candidates for example to explore many-body spin models from glassiness to associative memories [28] or to solve specific NP hard problems [29], as they are able to generate tunable-range interactions between atoms placed inside the cavities [25, 53, 54].

By way of an introduction think, however, of the simplest possible example, the Jaynes-Cummings model [55] consisting of a single two-level atom only. This is described by the choices

$$H_A = \frac{\omega}{2}\sigma_z, \quad L = \sigma_-, \quad (2)$$

where σ_α ($\alpha = x, y, z$) are the standard Pauli operators $\sigma_x = |0\rangle\langle 1| + |1\rangle\langle 0|$, $\sigma_y = i(|0\rangle\langle 1| - |1\rangle\langle 0|)$ and $\sigma_z = |1\rangle\langle 1| - |0\rangle\langle 0|$ with $|0\rangle$ and $|1\rangle$ the two relevant atomic states, separated by the atomic transition frequency ω . This model is particularly simple because the Hamiltonian conserves the total number of atomic excitations and photons. In order to gain information on the state of the atoms via the cavity field, the outgoing cavity field can be continuously monitored, for instance with homodyne detection. The joint atom-cavity time evolution is then conditioned on the measured homodyne current J_{hom} . For perfect detection efficiency, the detected signal can be written in the form [1]

$$J_{hom} dt = \sqrt{2\kappa}\langle a + a^\dagger \rangle dt + dW. \quad (3)$$

Throughout the paper, the brackets $\langle \dots \rangle$ denote the quantum expectation value with respect to the current conditioned state. The signal thus contains information on a particular quadrature of the mode. The second term that contributes to the homodyne current is white noise which arises due to the randomness of quantum measurement outcomes, written here in terms of increments dW of the Wiener process with zero mean $E[dW] = 0$, obeying Ito's rule $dW^2 = dt$. The measurement strength κ is determined by the rate of light leaking out from the cavity mirrors. Through continuous measurement, information on the joint system of cavity field and atoms is continuously acquired. Thus, the state of atoms and field ρ_{AC} is influenced by, or conditioned on, the measurement outcome and obeys the stochastic evolution equation [1]

$$\begin{aligned} d\rho_{AC} = & -i[H_{AC}, \rho_{AC}]dt + \kappa (2a\rho_{AC}a^\dagger - \{a^\dagger a, \rho_{AC}\})dt \\ & + \sqrt{2\kappa} ((a - \langle a \rangle)\rho_{AC} + \rho_{AC}(a^\dagger - \langle a^\dagger \rangle))dW. \end{aligned} \quad (4)$$

Note that here we may in fact have pure state solutions $\rho_{AC} = |\psi_{AC}\rangle\langle\psi_{AC}|$ (quantum trajectories, see later). To obtain the evolution of the average state, that is the average with respect to all measurement realizations, we

simply have to omit the terms involving the stochastic increment dW . We are left with the standard master equation of cavity decay in Gorini-Kossakowski-Sudarshan-Lindblad (GKSL), or Lindblad, form [56, 57]. The main goal of this work is to develop a theory describing the continuously monitored state of the atoms only, $\rho_A = \text{tr}_C \rho_{AC}$, by tracing out the cavity field in (4), without further approximation. It is clear that while the monitored ρ_{AC} may well be pure, ρ_A will almost always be mixed. In the next section we will derive our exact hierarchical scheme for non-Markovian quantum trajectories of the monitored, mixed ρ_A .

Before doing so, we discuss two known approaches, where the desired ρ_A is obtained through approximations: the simplest way is via adiabatic elimination – formally a second order perturbation theory in the coupling strength g , leading to an effective theory for the reduced state of the atoms described by the conditioned Redfield master equation

$$\begin{aligned} d\rho_A \approx & \left(-i[H_A, \rho_A] + [\bar{L}\rho_A, L^\dagger] + [L, \rho_A \bar{L}^\dagger] \right) dt \\ & + \frac{i}{g} \sqrt{2\kappa} \left((\rho_A (\bar{L}^\dagger - \langle \bar{L}^\dagger \rangle) - (\bar{L} - \langle \bar{L} \rangle) \rho_A) \right) dW. \end{aligned} \quad (5)$$

Here, the operator \bar{L} is time-dependent and given as

$$\bar{L}(t) = \int_0^t ds g^2 e^{-(i\Delta+\kappa)(t-s)} e^{-iH_A s} L e^{iH_A s}. \quad (6)$$

This equation is explicitly derived later in this work, and also in Ref. [48]. When the average over all measurement results is taken, i.e. the second line is neglected, equation (5) reduces to the deterministic Redfield master equation of atoms coupled to a non-Markovian reservoir with Lorentzian spectral density, reflecting the leaky cavity mode. Also, within the approximation, the measured homodyne current relates directly to the state of the atoms $J_{hom} dt \approx -i\frac{\sqrt{2\kappa}}{g} \langle \bar{L} - \bar{L}^\dagger \rangle dt + dW$, signaling that the cavity field is assumed to effectively follow the state of the atoms. The Redfield equation cannot capture strong memory effects which may occur in the interaction of the atoms with the cavity field. Recent work shows that for instance in the $U(1)$ -symmetric Dicke model, a higher order perturbative evolution equation is required to correctly capture the state of the atoms and the phase transition [58], while in the standard dissipative Dicke model Redfield theory does yield accurate results [59]. Hence, even in relatively simple models, it is not obvious how to eliminate the cavity modes appropriately. We will see later that Eq. (5) will drop out naturally as only the first order approximation in our general hierarchical approach.

On top of the weak-coupling limit leading to the Redfield theory, one can make further simplifications based on assumptions on the timescales of the cavity and atom processes. A popular approximation is the 'bad cavity' limit, where the cavity decay is assumed to be the fastest

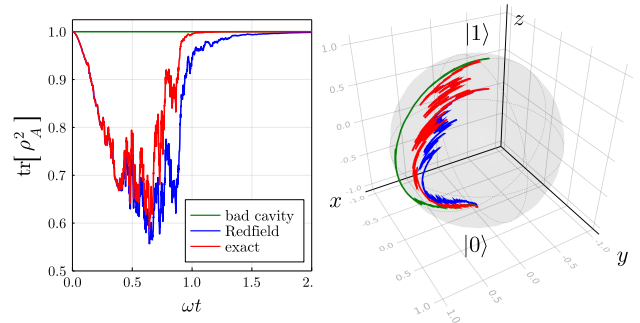


FIG. 2. Example of homodyning atomic trajectories for the Jaynes-Cummings model with $g = 2\omega$, $\Delta = \omega$ and $\kappa = 3\omega$ for different approximation schemes. Left: Purity of the atomic state $\text{tr}[\rho_A^2]$ as a function of time obtained in the bad cavity limit [green line, Eq. (7)], the Redfield limit [blue line, Eq. (5)] and the exact equation [red line, Eq. (4)]. As seen on the plot, in the bad cavity approximation the state is pure, which is not in agreement with the exact dynamics. Thus, in this approximation, the state of the atom remains on the Bloch sphere (right figure).

timescale $\kappa \gg \omega, \Delta$. Then we can approximate the Redfield operator as $\bar{L} \approx g^2 L / \kappa$ which leads to an effective stochastic master equation of the same form as (4),

$$\begin{aligned} d\rho_A \approx & -i[H_A, \rho_A] dt + \frac{g^2}{\kappa} (2L\rho_A L^\dagger - \{L^\dagger L, \rho_A\}) dt \\ & + \frac{ig\sqrt{2}}{\sqrt{\kappa}} ((L - \langle L \rangle) \rho_A + \rho_A (L^\dagger - \langle L^\dagger \rangle)) dW. \end{aligned} \quad (7)$$

In this approximation all memory effects of the cavity field vanish and the atoms obey GKSL-Lindblad dynamics.

To give an example we consider a single realization of the Jaynes-Cummings model conditioned on a given homodyne detection signal, shown in Fig. 2 as a trajectory on or inside the Bloch sphere. The dynamics in the Jaynes-Cummings model is simply a relaxation of the atomic excitation to the ground state, which is a stationary state. The different plots in the figure compare an exact solution of the Jaynes Cummings model via master equation (4) with the Redfield approximation (5) and the bad cavity limit (7). Clearly, the bad cavity limit is not applicable in this parameter regime. Note that, in contrast to the bad cavity limit, the true conditioned atomic state does not remain pure, as indicated by a purity $\text{tr}\rho_A^2(t)$ of less than one. This is because the atom-field interaction leads to finite entanglement between atom and the cavity mode. The Redfield approximation is close to the exact solution, but does not match perfectly even though, here, the cavity field can have at most a single photon occupation. This example highlights that a more systematic method is needed in order to compute the conditioned state of the atoms within an atom-only description.

III. ATOM-ONLY CONDITIONED HIERARCHICAL EQUATIONS OF MOTION

We can overcome the clear limitations of an adiabatic treatment of the environmental modes with a general and versatile non-Markovian theory which can account for continuous monitoring of the modes. In particular, we introduce a generalization of the hierarchical equations of motion (HEOM) method, a well established method for the numerical treatment of non-Markovian open quantum systems [51, 52, 60–62]. We develop this theory based on an ansatz presented already in Ref. [48], using ideas of non-Markovian quantum state diffusion [63–65]. In [48], the authors formulate a closed non-Markovian conditioned master equation via an operator replacement, which is feasible in special cases only, for instance when the full system is integrable. In contrast, hierarchy methods allow for a systematic expansion in terms of time-local evolution equations which can be readily integrated numerically. Such an expansion in the spirit of HEOM [51, 52] has been used in Ref. [66, 67] to include unmeasured non-Markovian environments of atoms in continuous measurement and feedback schemes where the measured cavity modes could, however, still be adiabatically eliminated. In the following we derive a conditioned hierarchy of equations of motion (cHEOM) that does not rely on any assumptions on the atom-cavity coupling or the cavity quality, and can include measured and unmeasured modes alike.

To sketch the derivation, we will focus on the simplest case of homodyne detection of the cavity output field from a single cavity mode only. The derivation of the various generalizations, which are presented later on, follows similar lines. For homodyne detection the joint atom and cavity state obeys the following stochastic Schrödinger equation [1, 68, 69], which is the pure state version of Eq. (4)

$$d|\psi_{AC}\rangle = \left(-iH_{AC} - \kappa a^\dagger a + \kappa \langle a + a^\dagger \rangle a \right) |\psi_{AC}\rangle dt + \sqrt{2\kappa} |\psi_{AC}\rangle dW + |\psi_{AC}\rangle d\mathcal{N}. \quad (8)$$

Here, $d\mathcal{N} = -\frac{\kappa}{4}(\langle a + a^\dagger \rangle)^2 dt - \frac{1}{2}\sqrt{2\kappa} \langle a + a^\dagger \rangle dW$ is a factor ensuring normalization. The pure conditioned states $|\psi_{AC}\rangle$ are standard Markovian quantum trajectories, and have a clear physical interpretation in terms of continuous measurement.

Non-Markovian generalizations of quantum trajectories are well known in the literature, for instance the non-Markovian version of quantum jumps [70, 71] and, more closely related to the results presented here, non-Markovian quantum state diffusion [63–65]. They have been used to compute the unmonitored dynamics of the atoms by propagating stochastic pure states. However, following [72–77], while a pure state solution of a general non-Markovian SSE can be interpreted as a conditioned state at any particular time [72, 73], joining up

these solutions to form a continuously monitored quantum trajectory is, up to special exceptions [42], generally impossible [75]. In our case, the joint atom-cavity quantum trajectory is Markovian, and, if pure, follows (8). We now aim to find an atom-only description of the non-Markovian dynamics of those atoms, leading to non-Markovian atomic quantum trajectories which are *mixed* states, and have a clear interpretation in terms of continuous measurement by construction.

In order to derive an equation for the state of the atoms, the cavity field in equation (8) must be traced out. For this we first project the equation onto a Bargmann coherent state of the cavity $|y\rangle = \exp(ya^\dagger)|0\rangle$, as in non-Markovian quantum state diffusion [63–65] or in Ref. [48], which yields

$$\begin{aligned} d\langle y|\psi_{AC}\rangle = & \\ & \left(-iH_A - ig(L^\dagger \partial_{y^*} + Ly^*) - (\kappa + i\Delta)y^* \partial_{y^*} \right. \\ & \left. + \kappa \langle a + a^\dagger \rangle \partial_{y^*} \right) dt \langle y|\psi_{AC}\rangle \\ & + \left(\sqrt{2\kappa} \partial_{y^*} dW + d\mathcal{N} \right) \langle y|\psi_{AC}\rangle \end{aligned} \quad (9)$$

To handle the derivative terms we define n -th order auxiliary states as $|\psi^{(n)}(y^*, t)\rangle = (gi\partial_{y^*})^n \langle y|\psi_{AC}(t)\rangle$ which themselves obey the coupled evolution equations

$$\begin{aligned} d|\psi^{(n)}\rangle = & \\ & \left(-iH_A - igLy^* - n(\kappa + i\Delta) \right) dt |\psi^{(n)}\rangle \\ & - \left(L^\dagger + \frac{i}{g} \kappa \langle a + a^\dagger \rangle - \frac{i}{g} (\kappa + i\Delta)y^* \right) dt |\psi^{(n+1)}\rangle \\ & + d\mathcal{N} |\psi^{(n)}\rangle - \frac{i}{g} \sqrt{2\kappa} dW |\psi^{(n+1)}\rangle \\ & + g^2 n L dt |\psi^{(n-1)}\rangle \end{aligned} \quad (10)$$

reminiscent of the hierarchy of pure states (HOPS) in non-Markovian quantum state diffusion [78, 79]. Here, however, we determine *conditioned* atomic states under continuous (homodyne) measurement of the cavity modes. As with HOPS, the reduced state of the atoms is recovered by taking a Gaussian average over the y^* variable upon acknowledging the completeness of coherent states with respect to a Gaussian measure

$$\begin{aligned} \rho_A(t) &= \text{tr}_C |\psi_{AC}(t)\rangle \langle \psi_{AC}(t)| \\ &= \int \frac{d^2y}{\pi} e^{-|y|^2} |\psi^{(0)}(y^*, t)\rangle \langle \psi^{(0)}(y^*, t)| \\ &\equiv E_y \left[|\psi^{(0)}(y^*, t)\rangle \langle \psi^{(0)}(y^*, t)| \right]. \end{aligned} \quad (11)$$

Note that ρ_A is the state of the atoms conditioned on the homodyne measurement record of the output field. Similar to [80], we can replace the hierarchy of conditioned pure states (10) by matrix hierarchical equations of motion for the y -averaged, conditioned auxiliary matrices

$$\rho_A^{(n,m)}(t) = E_y \left[|\psi^{(n)}(y^*, t)\rangle \langle \psi^{(m)}(y^*, t)| \right]. \quad (12)$$

To find a closed evolution equation for these objects one has to employ partial integration under the Gaussian y -mean, which allows to evaluate $E_y [ig|\psi^{(n)}(y^*, t)\rangle\langle\psi^{(m)}(y^*, t)|] = E_y [ig\partial_{y^*}|\psi^{(n)}(y^*, t)\rangle\langle\psi^{(m)}(y^*, t)|] = \rho_A^{(n+1,m)}(t)$. The resulting cHEOM reads

$$\begin{aligned} d\rho_A^{(n,m)} = & \\ & \left(-i[H_A, \rho_A^{(n,m)}] - [(n-m)i\Delta + (m+n)\kappa]\rho_A^{(n,m)} \right. \\ & + g^2 \left(nL\rho_A^{(n-1,m)} + m\rho_A^{(n,m-1)}L^\dagger \right) \\ & + \left[\rho_A^{(n+1,m)}, L^\dagger \right] + \left[L, \rho_A^{(n,m+1)} \right] \right) dt \\ & + \left(-\sqrt{2\kappa}\langle X \rangle \rho_A^{(n,m)} \right. \\ & \left. + \frac{i}{g}\sqrt{2\kappa} \left(\rho_A^{(n,m+1)} - \rho_A^{(n+1,m)} \right) \right) dW, \end{aligned} \quad (13)$$

a main result of our work. Here, arising from the measured homodyne current, a term $\langle X \rangle = \langle a + a^\dagger \rangle = \text{tr}(\rho_A^{(1,0)} - \rho_A^{(0,1)})/(ig)$ appears, that can be determined from the auxiliary matrices of first order. The zeroth order auxiliary state $\rho_A^{(0,0)}$ is the exact physical state of the atoms conditioned on the measurement record, as can be seen from Eq. (11). As the above equation is expressed in Ito formalism, it is written in terms of the stochastic increment dW , related to the physical measurement current via Eq. (3). For completeness, this main result is presented in the Stratonovich formulation of stochastic calculus in appendix A, where the explicit dependence on the actual measurement current J_{hom} becomes obvious.

To recover the unobserved average reduced atomic state, one additionally has to take the average over the homodyne current J_{hom} , which amounts to taking the average with respect to the increments dW in (13): one simply has to omit all terms proportional to dW . As could be expected, this yields the standard HEOM for a quantum system in a bath with Lorentzian spectral density [80]. Here, remarkably, we obtain HEOM from an entirely different, Markovian continuous measurement-based approach.

Clearly, the derivation can be straightforwardly generalized to other measurement schemes such as direct photodetection or heterodyne detection. This is shown in appendix B, where also the corresponding hierarchical equations are provided.

While the full hierarchy (13) is in principle exact, the main practical advantage of the cHEOM arises from the fact that it can be truncated at finite order, and the consistency of that truncation can be checked: depending on the excitation of the modes, only a few auxiliary states need to be taken into account. In fact, the trace of auxiliary states gives the moments of cavity operators via

$$\langle a^n(a^\dagger)^m \rangle(t) = \frac{\text{tr} \rho_A^{(n,m)}(t)}{(ig)^n(-ig)^m} \quad (14)$$

so that a neglect of high order auxiliary states amounts to neglecting corresponding higher order moments. As used earlier, Eq. (14) makes it possible to compute the homodyne current (3) from the first level auxiliary states. Note that in the following we consider an initial condition with no photons in the cavity, so that all higher order hierarchy states are initially zero. Their norm then increases over time, as the modes become occupied in the dynamics.

Nicely, a second order perturbation theory can be derived with ease from the full hierarchy by formally integrating the equations for the first level auxiliary states and neglecting all contributions of higher order. In this approximation, the first auxiliary states can be expressed as

$$\begin{aligned} \rho_A^{(1,0)}(t) &= \bar{L}(t)\rho_A^{(0,0)}(t), \\ \rho_A^{(0,1)}(t) &= \rho_A^{(0,0)}(t)\bar{L}^\dagger(t), \end{aligned} \quad (15)$$

where $\bar{L}(t)$ is the Redfield operator (6). Inserting this in the zeroth order equation of the hierarchy (13) gives the closed stochastic master equation for the conditioned state of the atoms (5). As expected, taking the average with respect to the increments dW results in the standard deterministic Redfield equation for a bath with Lorentzian spectral density. Equation (5) can thus be seen as a generalization of the Redfield theory to continuous measurement.

To showcase the developed cHEOM method, we go beyond the Jaynes-Cummings model (2) and include a driving term in the Hamiltonian $\frac{\varepsilon}{2}\sigma_x$. For a nonzero driving the number of excitations is no longer preserved and the hierarchy does not truncate at the second order. In Fig. 3 we show the convergence of the solutions with respect to the hierarchy depth, that is we simply truncate the hierarchy by setting $\rho_A^{(n,m)} = 0$ for $n + m$ larger than the maximal depth k_{\max} . The figure clearly shows how a truncated cHEOM gives a systematic expansion beyond Redfield theory which converges to the exact result, as the hierarchy depth is increased. In this case, the exact result can be obtained by directly solving Eq. (4) for the joint atom and cavity system.

Indeed, for this simple example with only a single cavity mode, solving the full Markovian stochastic master equation (4) is possible, and our hierarchical atom-only formulation is not required to numerically determine the atomic time evolution. In the following section we introduce a generalization of the hierarchy to multiple bath modes. In this case the cHEOM can open new possibilities to tackle the challenging description of cavity QED systems in multimode cavities.

IV. MULTIPLE CAVITY MODES

Exploiting the opportunities of multimode cavities or ensembles of coupled single-mode cavities experimentally has offered new fascinating possibilities for cavity QED

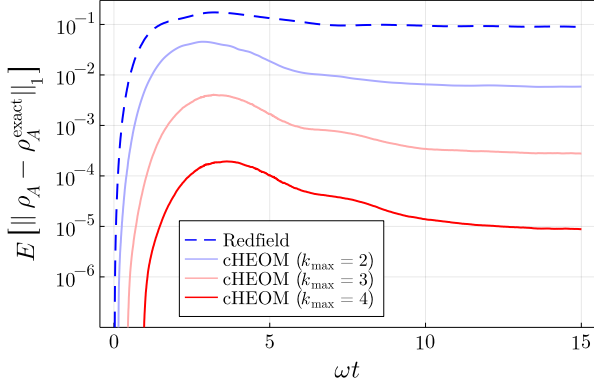


FIG. 3. Average trace distance $E[||\rho_A - \rho_A^{\text{exact}}||_1]$ of homodyning trajectories $\rho_A(t)$ [Eq. (13)] to the exact result $\rho_A^{\text{exact}}(t)$ for the driven Jaynes-Cummings model with $g = 2\omega$, $\varepsilon = 0.5\omega$, $\Delta = \omega$ and $\kappa = 2\omega$ using different approximation schemes, where $||O||_1 = \text{tr}\sqrt{O^\dagger O}$ denotes the trace norm of an operator O . The average is taken with respect to 1000 samples of the homodyne current and the initial state is $|1\rangle$.

physics simulations of many-body phenomena. The ex-

ponential size of the combined atom and cavity modes Hilbert space poses problems for a straightforward numerical treatment. Our cHEOM formalism can be generalized easily to multiple cavity modes which may or may not be continuously monitored by any of the measurement schemes discussed above, offering numerical advantages, as we shall see. The general Hamiltonian we like to consider reads

$$H = H_A + \sum_{k=1}^M g_k (L_k^\dagger a_k + L_k a_k^\dagger) + \Delta_k a_k^\dagger a_k. \quad (16)$$

Here, M cavity modes couple to the atoms with different strengths g_k and possibly different coupling operators L_k . For simplicity, we assume homodyne detection on all modes. In the multimode case the auxiliary density operators in the cHEOM acquire an index for each mode so that it is useful to define a vector notation where $\mathbf{n} = (n_k)$ and $\mathbf{m} = (m_k)$ are vectors of indices and $\mathbf{w} = (\kappa_k + i\Delta_k)$ is a vector storing the cavity mode detunings and decay rates. Then the cHEOM for the atom state conditioned on all homodyne currents $J_{hom,k}(t)$ reads

$$\begin{aligned} d\rho_A^{(\mathbf{n}, \mathbf{m})}(t) = & \left(-i[H_A, \rho_A^{(\mathbf{n}, \mathbf{m})}] - (\mathbf{w} \cdot \mathbf{n} + \mathbf{w}^* \cdot \mathbf{m}) \rho_A^{(\mathbf{n}, \mathbf{m})} \right) dt \\ & + \sum_{k=1}^M \left(g_k^2 \left(n_k L_k \rho_A^{(\mathbf{n}-\mathbf{e}_k, \mathbf{m})} + m_k \rho_A^{(\mathbf{n}, \mathbf{m}-\mathbf{e}_k)} L_k^\dagger \right) + \left[\rho_A^{(\mathbf{n}+\mathbf{e}_k, \mathbf{m})}, L_k^\dagger \right] + \left[L_k, \rho_A^{(\mathbf{n}, \mathbf{m}+\mathbf{e}_k)} \right] \right) dt \\ & + \sum_{k=1}^M \left(-\sqrt{2\kappa_k} \langle X_k \rangle \rho_A^{(\mathbf{n}, \mathbf{m})} + \frac{i}{g_k} \sqrt{2\kappa_k} \left(\rho_A^{(\mathbf{n}, \mathbf{m}+\mathbf{e}_k)} - \rho_A^{(\mathbf{n}+\mathbf{e}_k, \mathbf{m})} \right) \right) dW_k, \end{aligned} \quad (17)$$

one of the central results of our work. Here, we use the unit vectors $\mathbf{e}_k = (\delta_{kk'})$ and scalar product $\mathbf{a} \cdot \mathbf{b} = \sum_k a_k b_k$, and $\langle X_k \rangle = \langle a_k + a_k^\dagger \rangle = \text{tr}(\rho_A^{(\mathbf{e}_k, 0)} - \rho_A^{(0, \mathbf{e}_k)}) / (ig_k)$ arises from the homodyne current. In addition to taking into account multiple cavity modes with non-Markovian response, further Markovian dissipation channels of the atoms can be included simply by adding them to the hierarchy at each level. On the other hand also further non-Markovian baths could be accounted for by additionally employing any other suitable HEOM scheme, like the eHEOM method [81].

To demonstrate the applicability of our method to a nontrivial problem, we consider in the following a three-mode cavity where three localized 'clusters' of atoms are trapped. Each of the identical atoms in a particular cluster interacts with the cavity field in the same way, as sketched in Fig. 4(a). Then the interaction is collective and the cluster can be described by a large spin \vec{J}_i of size $j = N_{\text{atoms}}/2$. The atoms are assumed to interact with

the individual cavity modes according to a generalized Dicke Hamiltonian

$$H = \Omega \sum_{i=1}^{N_{\text{clusters}}} J_i^z + \Delta \sum_{k=1}^{N_{\text{modes}}} a_k^\dagger a_k + \sum_{ik} g_{ik} J_i^x (a_k + a_k^\dagger) \quad (18)$$

which can be realized by a double Raman pumping scheme [28, 82], and Markovian leakage of cavity photons with rate κ are assumed to be the only source of dissipation. Even for few cavity modes and moderate coupling, this system is numerically very challenging beyond an adiabatic regime where the cavity modes are either largely detuned or strongly damped. Thus it is a perfect setup to test the conditioned hierarchy (17).

As an interesting application, we study how monitoring of different cavity modes increases our knowledge about the state of the atoms in a single experimental run. This knowledge is quantified by the von-Neumann entropy of the state of the atoms $S[\rho_A] = -\text{tr}\rho_A \ln \rho_A$. In case a mode of the cavity field is continuously monitored, this entropy decreases. The expected information gain from the monitoring is given by the difference of the entropy

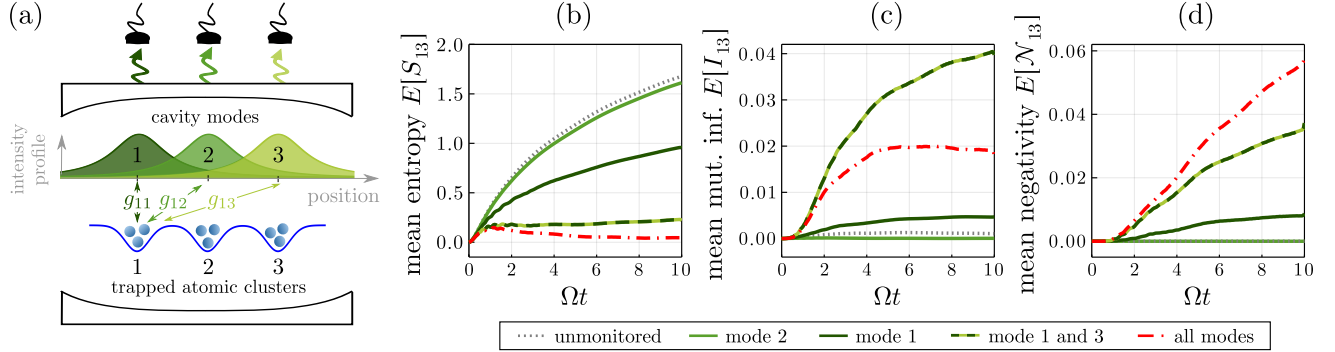


FIG. 4. Atomic dynamics in a lossy multimode cavity. (a) Sketch of a possible setup corresponding to Hamiltonian (18) and parameters (19), where three clusters of atoms are trapped in a plane transverse to the cavity axis and interact with cavity modes localized around the different clusters. Such spatial-dependent intensity profiles could be obtained in a confocal cavity QED [23, 25]. We assume that each cavity mode can be monitored independently. The panels (b), (c) and (d) show respectively the mean entropy, the mutual information and the negativity of the combined state of atomic cluster 1 and 3 depending on which modes of the cavity are continuously monitored via homodyning. The results are obtained from integrating 3000 samples of the conditioned HEOM (17) with parameters (19)–(21) and $N_{atoms} = 3$.

of the average state $S[E[\rho_A]]$ and the mean entropy of the conditioned states $E[S[\rho_A]]$ [10, 83]. The latter is a nontrivial nonlinear average of conditioned states which cannot be expressed by the reduced state, i.e. it is a property of the full ensemble and not just its mean. Thus it can only be evaluated by actually solving the full stochastic master equation for many different noise realizations. For an example calculation we choose three cavity modes and the following parameters

$$\Delta = \Omega/2, \quad (19)$$

$$\kappa = 2\Omega, \quad (20)$$

$$g = \begin{pmatrix} 0.4 & 0.115 & 0.003 \\ 0.115 & 0.4 & 0.115 \\ 0.003 & 0.115 & 0.4 \end{pmatrix} \Omega, \quad (21)$$

which are far from an adiabatic regime. The coupling is chosen such that each cavity mode is localized around a single cluster in a way that the coupling strength decays towards neighboring clusters. This induces an effective interaction between the clusters, mediated by a common coupling to the cavity field. In particular, we focus on the combined state of the first and last cluster given by $\rho_{13} = \text{tr}_2(\rho_A)$, where tr_2 denotes the trace over the second cluster. Fig. 4(b) shows the average entropy $E[S_{13}] \equiv E[S[\rho_{13}]]$ of the state ρ_{13} depending on which modes of the cavity field are continuously monitored by homodyning. As should be, the more modes are monitored the more information is gained on the state and the lower the mean entropy. Because the atom clusters become entangled with the cavity modes and the cluster 2, the entropy is nonzero even if all modes are monitored. Note that, interestingly, monitoring mode 2, which is localized around atom cluster 2, does not give a significant information gain on the state of cluster 1 and 3, compared to measuring modes localized around the latter.

As a second question of interest, we can study how the monitoring affects our knowledge on correlations be-

tween the clusters, characterized by the mutual information $I_{13} = S[\rho_1] + S[\rho_3] - S[\rho_{13}]$ between the first and the third cluster [10]. As seen in Fig. 4(c), showing the average mutual information $E[I_{13}]$, barely any correlations between cluster 1 and 3 are present in case none of the modes is monitored. In contrast, in case both mode 1 and 3 are monitored with homodyning, significant correlations between the clusters are expected in the individual experimental realizations. If in addition also mode 2 is monitored, these correlations decrease again. Note however, that quantum correlations cannot increase from neglecting the measurement results of mode 2. This means that the increase in mutual information in the case where mode 2 is not monitored, versus the case where all modes are monitored, is exclusively due to classical correlations.

The third question we like to address is how quantum correlations between clusters 1 and 3 are affected by the monitoring. Specifically, we quantify this by the negativity $\mathcal{N}_{13} \equiv \mathcal{N}[\rho_{13}] = (\|\rho_{13}^{\Gamma_1}\|_1 - 1)/2$ [84], where $\rho_{13}^{\Gamma_1}$ denotes the partial transpose of ρ_{13} with respect to the first cluster and $\|O\|_1 = \text{tr}\sqrt{O^\dagger O}$ the trace norm of an operator O . In Fig. 4(d), showing the mean negativity $E[\mathcal{N}_{13}]$, we observe how the completely monitored state contains the most negativity and then how it decreases when modes 1 and 3 and mode 1 alone are monitored. This is explained by the fact that quantum correlations cannot increase by classical averaging. When mode 2 alone or none of the modes are monitored, the state contains no negativity.

The effectiveness of our approach can be assessed when contrasted to the problem size when the cavity mode Hilbertspace would be directly truncated. The size of the space of the density matrices of the atomic system is $r = (2j + 1)^{2N_{\text{clusters}}}$. Using our approach and truncating the hierarchy according to a triangular condition $\sum_{k=1}^{N_{\text{modes}}} (m_k + n_k) \leq k_{\max}$ where m_k, n_k are the hierar-

chy indices results to total of K auxiliary density matrices with

$$K = \frac{(2N_{\text{modes}} + k_{\max})!}{(2N_{\text{modes}})!k_{\max}!}. \quad (22)$$

Thus, we need to solve a total of $d = rK$ equations. A direct truncation of the Fock space of the modes at k_{\max} leads to a full state dimension of $D = r(k_{\max} + 1)^{2N_{\text{modes}}}$. For $k_{\max} = 3$ we have $K = 84$ and this already gives two orders of magnitude reduction in the problem size $d/D = 84/4096 \approx 0.02$. This reduction becomes even more dramatic when the number of modes is increased or the modes are coupled more strongly. Further improvements could be achieved with advanced truncation procedures as in Refs. [79, 85].

V. FEEDBACK

From an experimental perspective, measuring single quantum trajectories is in general not feasible, as a particular trajectory cannot be prepared twice and any averaging required to reconstruct the state will reduce to the unmeasured case. This is different in case the measurement record is used as a feedback signal, which adjusts for instance the strength of a classical driving of the system. Then, average measurement results are predicted by a feedback master equation which deviates from the dynamics without feedback. Our formalism can be straightforwardly generalized to include feedback on the system based on continuous measurement. Here, we present such a theory in the simplest case of instantaneous feedback applied on the atomic system, but other generalizations such as delayed feedback can be derived similarly, following e.g. Ref. [1]. We want to consider in the following instantaneous feedback based on the homodyne signal of mode k . This corresponds to the feedback Hamiltonian

$$H_{fb}(t) = J_{hom,k}(t)F_k(t) \quad (23)$$

where F_k is an Hermitian operator which may be time-dependent. We restrict ourselves to the case where the feedback is applied to the atoms, so that F_k is an operator in the atom Hilbert space. It could, for instance, describe an external driving controlled by the experimenter. In the Stratonovich formulation of the conditioned HEOM provided in supplement A, the feedback can be trivially included simply by modifying the atom Hamiltonian accordingly. This can be converted to the Ito formalism which then allows to take the ensemble average. As shown in appendix C, the following contribution to the conditioned HEOM (17) arises due to the

feedback on mode k :

$$\begin{aligned} d_{fb}\rho^{(\mathbf{n},\mathbf{m})} = & \left(F_k \rho_A^{(\mathbf{n},\mathbf{m})} F_k - \frac{1}{2} \{ F_k^2, \rho_A^{(\mathbf{n},\mathbf{m})} \} \right. \\ & + \frac{\sqrt{2\kappa_k}}{g_k} \left([\rho_A^{(\mathbf{n}+\mathbf{e}_k,\mathbf{m})}, F_k] + [F_k, \rho_A^{(\mathbf{n},\mathbf{m}+\mathbf{e}_k)}] \right) \Big) dt \\ & - i[F_k, \rho_A^{(\mathbf{n},\mathbf{m})}] dW_k \end{aligned} \quad (24)$$

Most relevant is the feedback master equation, i.e. the equation for the averaged state. Again, in the Ito formalism, it is obtained by simply omitting all stochastic terms.

As an example, we apply the formalism to achieve unconditioned spin squeezing of an atomic system in a single-mode cavity via feedback of the homodyne current, following [13, 86]. The results in Ref. [13], however, have been obtained for the bad cavity limit, where an adiabatic elimination of the cavity mode can be performed. By contrast, our approach allows us to study the case of a 'good' cavity and we demonstrate the possibility of achieving squeezing for longer times in this regime. This example shows that our formalism opens possibilities to investigate quantum state preparation in strong coupling regimes without any restrictions on cavity parameters. A detailed discussion of this example follows.

As in [13, 87], we consider a system of N_{atoms} two-level atoms (spin-1/2) collectively coupled to a single mode of a lossy cavity described by the Hamiltonian

$$H = \Omega J_z - ig J_z (a - a^\dagger), \quad (25)$$

similar to the generalized Dicke Hamiltonian introduced in Eq. (18). In the following we consider $N_{\text{atoms}} = 10$ and $g = \Omega/2$.

We assume that initially, the state of the atoms is a coherent spin state with all spins aligned along the direction x . The output field is measured via homodyning – in a second step, the current is then fed back according to (23).

Since the coherent state is a minimum uncertainty state, the initial variances along the directions z and x are equal to $j/2 = N_{\text{atoms}}/4$. As we will see below, the continuous measurement reduces the uncertainty along z , hence generating spin squeezing, which we quantify using the spin squeezing parameter [88, 89]

$$\xi_z^2 = N_{\text{atoms}} \frac{(\Delta J_z)^2}{\langle J_x \rangle^2 + \langle J_y \rangle^2}. \quad (26)$$

However, the spin squeezing of the conditioned states disappears after carrying out the ensemble average over all possible measurement records, because of the presence of a stochastic shift of $\langle J_z \rangle$ which returns the unconditioned initial variance. Therefore, as in Ref. [13], one introduces a coherent feedback based on the measurement to counteract this stochastic shift, in order to maintain the spin squeezing. Our goal here is to apply this idea to achieve

such spin squeezing in the good cavity limit, where the cavity mode cannot be eliminated. We will see that the feedback conditioned on the measurement will then not depend on quantities of the atoms only, but on quantities of both the atoms and the cavity, and more precisely on their correlations, as we show in the following.

From the general form of the Hamiltonian as in Eq. (1) we can identify the correspondence

$$\begin{aligned} H_A &= \Omega J_z, \\ L &= iJ_z, \\ \Delta &= 0. \end{aligned} \quad (27)$$

A continuous measurement produces a stochastic shift of the z component $\langle J_z \rangle$. Using the conditioned HEOM equation (13), as well as (14), we find that this shift is given by

$$\begin{aligned} d\langle J_z \rangle &= \text{Tr}[J_z d\rho_A] \\ &= \sqrt{2\kappa}(\langle J_z X \rangle - \langle J_z \rangle \langle X \rangle) dW, \end{aligned} \quad (28)$$

where we used the quadrature $X = a + a^\dagger$. From the homodyne current in Eq. (3) we can extract the form of dW and use this in Eq. (28), obtaining

$$d\langle J_z \rangle = \sqrt{2\kappa} dt(\langle J_z X \rangle - \langle J_z \rangle \langle X \rangle)(J_{hom}(t) - \sqrt{2\kappa} \langle X \rangle), \quad (29)$$

which, using the fact that $\langle X \rangle = 0$ (as shown in Figure 5), simplifies to

$$d\langle J_z \rangle = \sqrt{2\kappa} \langle J_z X \rangle J_{hom}(t) dt. \quad (30)$$

In the absence of feedback, this stochastic shift, averaged over all the trajectories, will return a final non squeezed state, recovering the unconditioned variance for J_z with the same value $j/2$ of the initial coherent state. This shift induced by the measurement is hence detrimental for the spin squeezing along z and must be counteracted with an additional feedback term that continuously acts on the system and induces an opposite shift of $\langle J_z \rangle$.

Following the same protocol as in [13], we add a feedback that generates a rotation of the collective spin around the y axis:

$$H_{fb}(t) = \frac{\lambda(t)}{\sqrt{2\kappa}} J_{hom}(t) J_y = F J_{hom}(t), \quad (31)$$

where we defined the feedback operator

$$F = \frac{\lambda(t)}{\sqrt{2\kappa}} J_y, \quad (32)$$

and where λ is the feedback strength. As the feedback Hamiltonian adds the extra terms (24) to the conditioned HEOM, the feedback induces another shift on $\langle J_z \rangle$

$$d_{fb}\langle J_z \rangle = -\frac{\lambda(t)}{\sqrt{2\kappa}} J_{hom}(t) \langle J_x \rangle dt. \quad (33)$$

For the total stochastic shift to vanish for a single trajectory, we have to impose $d\langle J_z \rangle = 0$. From Eq. (30) and Eq. (33) we therefore obtain the condition on the feedback strength

$$\lambda(t) = 2\kappa \frac{\langle J_z X \rangle}{\langle J_x \rangle}. \quad (34)$$

It is worth highlighting that the feedback strength in Eq. (34) depends dynamically on conditioned expectation values of both a quantity of the atomic system alone, J_x , and of a quantity that is related to the correlations between atoms and cavity, $J_z X$, as shown in Fig. 5. Note that we can directly extract the relevant expectation value from the hierarchy (17) as

$$\langle J_z X \rangle = i/g \text{Tr} \left(J_z (\rho_A^{(1,0)} - \rho_A^{(0,1)}) \right). \quad (35)$$

In the bad cavity limit, where the cavity mode can be adiabatically eliminated, one can set optimised values for the feedback strength under the assumptions that perfect measurements on the system keep it in a pure state, so that the conditioned expectation values can be approximated with the unconditioned ones (indicated with the subscript u): $\langle J_x \rangle \simeq \langle J_x \rangle_u$ and $\langle J_z^2 \rangle \simeq \langle J_z^2 \rangle_u$ [87].

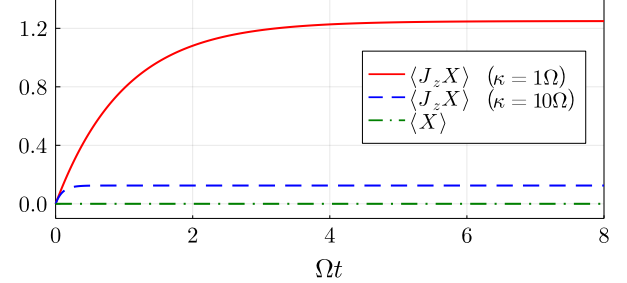


FIG. 5. Time-dependent behavior of the correlations $\langle J_z X \rangle$ for two different values of the cavity loss rate $\kappa = \Omega$ (solid red line) and 10Ω (dashed blue line) – corresponding respectively to the good and bad cavity regimes – and of $\langle X \rangle$ (dashed dotted green line) for both values of κ . While the quadrature $\langle X \rangle$ remains zero for all times in both regimes, correlations between the atoms and the cavity mode build up. The smaller κ , the larger the correlations.

In the good cavity limit, however, the state becomes mixed, and we determine the optimal values of the feedback strength numerically. While we could choose a time-dependent feedback, determining this would not be practical in an experimental setup. We therefore consider the simpler situation of constant feedback applied throughout the dynamics, using different values of the feedback strength λ within a given range, to see which values optimize the spin squeezing along z , Eq. (26). This is shown

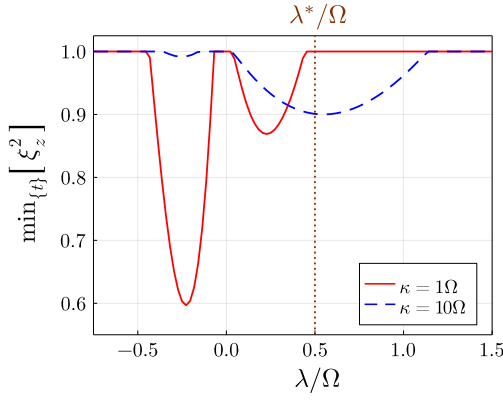


FIG. 6. Minimum spin squeezing parameter ξ_z^2 obtained over time as a function of constant feedback strength for two different values of κ that corresponds to the good ($\kappa = \Omega$, red solid line) and bad ($\kappa = 10\Omega$, blue dashed line) cavity regimes. Better spin squeezing is achieved in the good cavity regime. The brown dashed line indicates the feedback strength $\lambda^* = 2\kappa \max_{\{t\}} \langle J_z X \rangle / \langle J_x(0) \rangle$, which is evaluated using the maximum of $\langle J_z X \rangle$ over time (shown in Fig. 5), and takes the same value for both $\kappa = \Omega$ and $\kappa = 10\Omega$. The values $\lambda_{-,-+}^{(\kappa/\Omega)}$ of the feedback strength corresponding to the negative and positive minima, in the good and bad cavity limit, are: $\lambda_-^{(1)} = \lambda_-^{(10)} = -0.22\Omega$, $\lambda_+^{(1)} = 0.23\Omega$ and $\lambda_+^{(10)} = 0.55\Omega$.

in Fig. 6 for both the good (red line) and bad (blue line) cavity limits.

First, we can observe that the good cavity case, in this regime of parameters, produces better spin squeezing. Second, while for the bad cavity regime, considering a feedback strength λ^* set by the maximum of the correlations $\langle J_z X \rangle$ is a good approximation, this is not true in the good cavity limit. In fact, if we use this approximation to set the value of the feedback strength, we do not obtain any spin squeezing, and this is due to two factors: first, the correlations are stronger and grow more slowly (as shown in Figure 5), introducing a limitation of the approximation to a constant value; second, in the good cavity limit the state of the system gets mixed quickly and the conditioned values obtained from the measurement differ from the unconditioned ones that we use to define the constant feedback strength. Fig. 6 also shows that in both the good and bad cavity limits, when we consider the full model, we have two local minima corresponding to values of λ having different signs. It is worth pointing out that if we adiabatically eliminate the cavity mode, for the same values of the parameters used here, we would obtain only one of the two minima and the physics of the second minimum would not be captured in this approximation.

The constant feedback applied with strengths set by the different values of the minima in Fig. 6 generates spin squeezing at different points in time, as can be observed from the dashed lines in Fig. 7. We can exploit this to contrast the increase of the the spin squeezing parameter after a transient [13] and decrease it further for longer

times, by using a sequence of the optimal constant feedback strengths with different signs, switching from one to another at given times. The result is shown by the solid lines in Fig. 7.

Note that while our approach provides a simple physical picture of the mechanism leading to a better spin squeezing, one could potentially improve further these results by optimizing a continuous time-dependent feedback strength $\lambda(t)$ via optimal control schemes. However, from an experimental point of view, this would be much harder to implement.

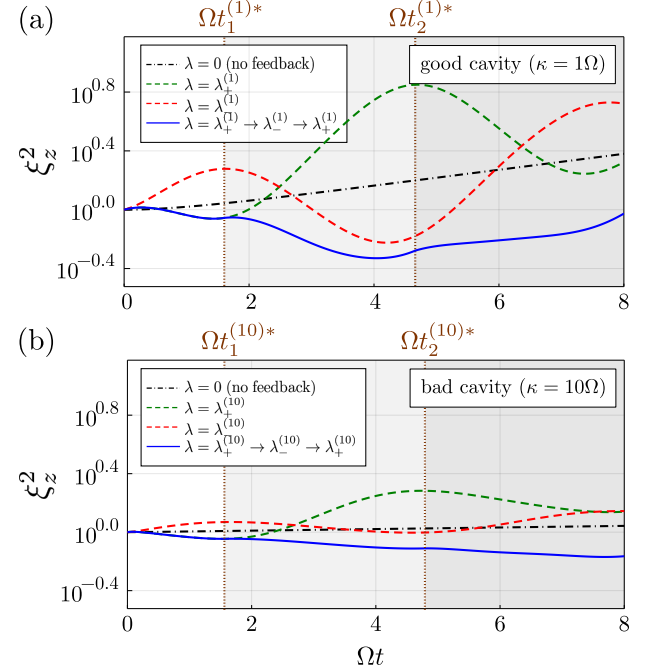


FIG. 7. Spin squeezing obtained applying the feedback of Eq. (31) with different feedback strengths, for the good [top, panel (a)] and bad [bottom, panel (b)] cavity regimes $\kappa = \Omega$ and $\kappa = 10\Omega$ respectively. The green (red) dashed line is obtained when we apply the feedback with the optimal positive (negative) feedback parameter $\lambda_{+(-)}^{(\kappa/\Omega)}$ coherently from $t = 0$. The maximum spin squeezing is obtained at $\Omega t = 4$ and $\Omega t \sim 1.8$ for the good and bad cavity limits respectively. The blue solid line is the spin squeezing parameter where we alternate the positive and negative feedback following the sequence: $\lambda_+^{(\kappa/\Omega)} \rightarrow \lambda_-^{(\kappa/\Omega)} \rightarrow \lambda_+^{(\kappa/\Omega)}$, where the switching occurs at times $t_1^{(\kappa/\Omega)*}$ and $t_2^{(\kappa/\Omega)*}$. Here we have $\Omega t_1^{(1)*} = \Omega t_1^{(10)*} = 1.6$, $\Omega t_2^{(1)*} = 4.66$ and $\Omega t_2^{(10)*} = 4.81$.

VI. CONCLUSIONS AND OUTLOOK

In this article we have developed a general theory describing the time evolution of a non-Markovian subsystem coupled to damped bosonic modes which are monitored continuously. This appears in many scenarios, including advanced cavity QED where multiple cavity

modes couple to an interacting many-body quantum system (atoms) embedded in the cavity. We address the problem which information about the atoms can be inferred from continuous measurement of the leaking output light of the various cavity modes, and how that knowledge can be used to manipulate the many-body state using feedback. We refrain from using any of the usual approximations but succeed in formulating a theory that allows us to determine directly the exact, non-Markovian atomic (mixed) state dynamics, conditioned on the measurement record. We can thus study in detail the gradual information gain arising from monitoring more and more cavity modes. We show how the continuous observation of spatially selective cavity modes reveals information about (quantum) correlations between groups of atoms at different locations inside the cavity. Moreover, we can determine non-Markovian feedback hierarchical equations of motion as a starting point for control theory, allowing us to drive the many-body quantum system in desired states. Specifically, we consider a feedback scenario which aims to generate spin squeezing in a collective ensemble of atoms. Here, the mixedness of the conditioned atom state invalidates the previously known optimal feedback protocols of the adiabatic regime. In fact, with a more coherent cavity it is possible to generate stronger spin squeezing for significantly longer times.

Crucially, in our approach, no restrictions on coupling strengths or cavity qualities are required. Instead, our result takes the form of conditioned hierarchical equations of motion (cHEOM, Eq. (17)), proving to be an efficient scheme for tackling pressing issues in the highly complex quantum dynamics of strong atom-cavity coupling.

Our result paves the way for further exciting routes of study: our exact cHEOM could be naturally coupled to approximated schemes such as mean-field or cumulant expansion, to easily go towards larger many-body atomic systems while keeping the system-reservoir coupling exact. It could also be advantageous to formulate cHEOM with matrix product operators. In connection with the hierarchy of pure states method, recent works have demonstrated that such an ansatz can be used both to describe many-body dynamics in non-Markovian environments [36] and very strong system-bath coupling [90].

Our theory constitutes an ideal framework for the exploration of a wide range of many-body phenomena on the level of the reduced atomic non-Markovian dynamics in the strong-coupling regime, such as phase transitions [91], measurement-induced phase transitions [92, 93], neural network like behaviors such as associative memories [28, 94], cavity-enhanced transport [95–99] and superconductivity [100], continuous measurement of transport [101], or cavity cooling with higher capture range [102] and its monitoring [103]. New schemes for quantum information processing and production of entanglement [32] could also be investigated, exploiting the higher coherence achievable in the strong-coupling regime, the use of different cavity modes to realize quantum gates (or conversely the use of the atoms to realize

quantum gates between photonic qubits [104, 105]), or the potential of using the feedback formalism to implement error correction protocols. Finally, it is important to stress again that while we use the language of optical cavity QED, the underlying model is universal and can equally be applied to plasmonic cavities [40], cold atoms reservoirs [37–39], electron-phonon systems [36], or circuit QED [33, 35]. Given the high cooperativity achievable in this latter platform, we expect our formalism to be indeed particularly useful for exploring control and readout of superconducting qubits.

ACKNOWLEDGMENTS

It is a pleasure to thank Richard Hartmann and Stuart Flannigan for various helpful discussions in connection with this work. Work at the University of Strathclyde was supported by the EPSRC Programme Grant DesOEQ (EP/P009565/1), the European Union’s Horizon 2020 research and innovation program under grant agreement No. 817482 PASQuanS, and AFOSR grant number FA9550-18-1-0064. V. L. , F. D., W. S. and A. D. thank KITP for hospitality during this work, supported by the National Science Foundation under Grant No. NSF PHY-1748958.

Appendix A: Homodyne cHEOM in Stratonovich convention

To derive the Stratonovich from of equation (13) we start from the conditioned atom and cavity evolution in Stratonovich convention [1, 69]

$$\partial_t |\psi\rangle = \left(-iH_A - ig(L^\dagger a + La^\dagger) - (\kappa + i\Delta)a^\dagger a - \kappa a^2 + \sqrt{2\kappa}J_{hom}(t)a + \mathcal{N}(t) \right) |\psi\rangle, \quad (A1)$$

where $\mathcal{N}(t) = \kappa(\langle a^\dagger a \rangle + 1/2\langle a^2 + (a^\dagger)^2 \rangle) - \sqrt{\kappa/2}J_{hom}(t)\langle a + a^\dagger \rangle$ is a factor which ensures normalization. The measured homodyne current is given as

$$J_{hom}(t) = \sqrt{2\kappa}\langle a + a^\dagger \rangle_J(t) + \zeta(t), \quad (A2)$$

where $\zeta(t)$ is a Gaussian white noise process in the Stratonovich sense with statistics $E[\zeta(t)] = 0$ and $E[\zeta(t)\zeta(s)] = \delta(t-s)$. In order to obtain the hierarchy we follow the same derivation as in section III, to

arrive at the Stratonovich version of Eq. (13)

$$\begin{aligned}
\partial_t \rho_a^{(n,m)}(t) = & \\
& -i[H_A, \rho_a^{(n,m)}] - [(n-m)i\Delta + (m+n)\kappa] \rho_a^{(n,m)} \\
& + g^2 (nL\rho_a^{(n-1,m)} + m\rho_a^{(n,m-1)} L^\dagger) \\
& + [\rho_a^{(n+1,m)}, L^\dagger] + [L, \rho_a^{(n,m+1)}] \\
& + \frac{i}{g} \sqrt{2\kappa} J_{hom}(t) (\rho_a^{(n,m+1)} - \rho_a^{(n+1,m)}) \\
& + \frac{\kappa}{g^2} (\rho_a^{(n+2,m)} + \rho_a^{(n,m+2)} - 2\rho_a^{(n+1,m+1)}) \\
& - 2 \operatorname{Re}(\mathcal{N}(t)) \rho_a^{(n,m)}. \tag{A3}
\end{aligned}$$

The advantage of the Stratonovich formulation is that it becomes obvious that the state depends on the homodyne current (A2) only. Similarly, the second order perturbation theory equation (5) is equivalent to the following Stratonovich equation

$$\begin{aligned}
\partial_t \rho_a = & -i[H_A, \rho_a] + [\bar{L}\rho_a, L^\dagger] + [L, \rho_a \bar{L}^\dagger] \\
& + \frac{i}{g} \sqrt{2\kappa} J_{hom}(t) (\rho_a \bar{L}^\dagger - \bar{L}\rho_a(t)) \\
& + \frac{\kappa}{g^2} (\bar{L}^2 \rho_a(t) + \rho_a (\bar{L}^\dagger)^2 - 2\bar{L}\rho_a(t)\bar{L}^\dagger) \\
& - 2 \operatorname{Re}(\mathcal{N}(t)) \rho_a, \tag{A4}
\end{aligned}$$

which reduces to a Redfield master equation on average.

Appendix B: Different Detection Schemes

The derivations in section III can be straightforwardly applied to different measurement schemes. For example the formally very similar continuous heterodyne detection of the cavity output field yields the stochastic Schrödinger equation [1, 68]

$$\begin{aligned}
d|\psi(t)\rangle = & \left(-iH_A - ig(L^\dagger a + La^\dagger) \right. \\
& \left. - \kappa (\langle a^\dagger \rangle \langle a \rangle - 2\langle a^\dagger \rangle a - a^\dagger a) \right) |\psi(t)\rangle dt \\
& + \sqrt{2\kappa} (a - \langle a \rangle) |\psi(t)\rangle dW_c(t). \tag{B1}
\end{aligned}$$

This describes the evolution of atom and cavity state conditioned on the heterodyne current

$$J_{het}(t) dt = \sqrt{2\kappa} \langle a \rangle dt + dW_c, \tag{B2}$$

with the now complex Gaussian increment dW_c , whose stochastic properties are given by $E[dW_c] = dW_c dW_c = 0$ and $dW_c dW_c^* = dt$. The HEOM in this case reads

$$\begin{aligned}
d\rho_a^{(n,m)} = & \left(-i[H_A, \rho_a^{(n,m)}] - ((m-n)\Delta + (m+n)\kappa) \rho_a^{(n,m)} \right. \\
& + g^2 (nL\rho_a^{(n-1,m)} + m\rho_a^{(n,m-1)} L^\dagger) \\
& + [\rho_a^{(n+1,m)}, L^\dagger] + [L, \rho_a^{(n,m+1)}] \\
& + \sqrt{2\kappa} (-\langle a \rangle dW - \langle a^\dagger \rangle dW^*) \rho_a^{(n,m)} \\
& \left. + \frac{i\sqrt{2\kappa}}{g} \rho_a^{(n,m+1)} dW \frac{i\sqrt{2\kappa}}{g} \rho_a^{(n+1,m)} dW^* \right) \tag{B3}
\end{aligned}$$

Another well known unraveling of master equation (16) are quantum jumps which are related to continuous direct photodetection [1, 68]. In this case the conditioned evolution is piecewise deterministic until at a random time a photon is detected and the state jumps discontinuously. An evolution equation describing this can be formulated as follows

$$\begin{aligned}
d|\psi(t)\rangle = & -iH_A |\psi(t)\rangle dt \\
& \left(-ig(L^\dagger a + La^\dagger) - (\kappa + i\Delta) a^\dagger a - \kappa \langle a^\dagger a \rangle_N \right) |\psi(t)\rangle dt \\
& + \left(\frac{a}{\sqrt{\langle a^\dagger a \rangle_N(t)}} - 1 \right) |\psi(t)\rangle dN(t). \tag{B4}
\end{aligned}$$

Here, $dN(t)$ is the increment of a realization of a Poisson process obeying

$$E[dN] = 2\kappa \langle a^\dagger a \rangle_N dt, \quad (dN)^2 = dN. \tag{B5}$$

Clearly, dN can be either one or zero, depending on whether a jump does or does not occur. To realize this in a numerical implementation one first draws a random number r between 0 and 1 and then evolves the state according to the deterministic part of Eq. (B4). Then a jump occurs when $\int_0^t ds 2\kappa \langle a^\dagger a \rangle_N(s) = -\ln r$ is satisfied and the state loses one photon $|\psi\rangle \rightarrow a|\psi\rangle/\sqrt{\langle a^\dagger a \rangle_N}$. For the direct photodetection the hierarchy of equations of motion reads

$$\begin{aligned}
d\rho_a^{(n,m)} = & \left(-i[H_A, \rho_a^{(n,m)}] - ((n-m)i\Delta + (m+n)\kappa) \rho_a^{(n,m)} \right. \\
& + g^2 (nL\rho_a^{(n-1,m)} + m\rho_a^{(n,m-1)} L^\dagger) \\
& + [\rho_a^{(n+1,m)}, L^\dagger] + [L, \rho_a^{(n,m+1)}] \left. \right) dt \\
& + \left(2\kappa \langle a^\dagger a \rangle_N(t) \rho_a^{(n,m)} - 2\kappa \frac{1}{g^2} \rho_a^{(n+1,m+1)} \right) dt \\
& + \left(\frac{1}{g^2 \langle a^\dagger a \rangle_N(t)} \rho_a^{(n+1,m+1)} - \rho_a^{(n,m)} \right) dN(t). \tag{B6}
\end{aligned}$$

One can check immediately that the last two lines drop out after taking the average with relations (B5) and the standard HEOM is recovered again. If a jump occurs

then the hierarchy has to be modified according to

$$\rho_a^{(n,m)}(t) \rightarrow \frac{\rho_a^{(n+1,m+1)}(t)}{g^2 \langle a^\dagger a \rangle_N(t)}, \quad (\text{B7})$$

i.e. the entire hierarchy is moving down one level.

Appendix C: Homodyne cHEOM with feedback

To derive a HEOM that includes feedback we start from the SSE in Stratonovich convention as described in appendix A. There the rules for stochastic integration allow to simply add the feedback Hamiltonian (31), which describes linear feedback based on the measurement of a single mode k . We obtain

$$\begin{aligned} \partial_t |\psi\rangle = & \left(-i(H_A + J_{hom,k}F_k) - i \sum_j g_j (L^\dagger a_j + L a_j^\dagger) \right. \\ & + \sum_j -(\kappa_j + i\Delta_j) a_j^\dagger a_j - \kappa_j a_j^2 \\ & \left. + \sum_j \sqrt{2\kappa_j} J_{hom,j}(t) a_j + \mathcal{N}(t) \right) |\psi\rangle. \end{aligned} \quad (\text{C1})$$

As we consider only feedback on the atoms F_K is an operator in the system Hilbert space. From Eq. (A2) we see that the above SSE depends on the real noise $\zeta(t)$. To convert it into Ito formalism one can then take an arbitrary basis, define $\psi_j = \langle j|\psi\rangle$, $L_{j,k} = \langle j|L|k\rangle$ and make use of the conversion formula [69] for a Stratonovich equation of the form

$$\partial_t \psi_j = \alpha_j + \beta_j \zeta(t).$$

This Stratonovich equation is then translated to the Ito equation

$$d\psi_j = \alpha_j dt + \beta_j d\zeta + \frac{dt}{2} \sum_l \left(\beta_l \frac{\partial}{\partial \psi_l} \beta_j + \beta_l^* \frac{\partial}{\partial \psi_l^*} \beta_j \right).$$

Applied to (C1) we arrive at the following SSE with feedback in Ito form:

$$\begin{aligned} d|\psi\rangle = & \left(-i \left(H_A + \sum_j g_j (L^\dagger a_j + L a_j^\dagger) + \Delta_j a_j^\dagger a_j \right) \right. \\ & + \sum_l -\kappa_l \left(a_l^\dagger a_l - \langle a_l^\dagger + a_l \rangle a_l + \langle a_l + a_l^\dagger \rangle^2 / 4 \right) \\ & \left. - i\sqrt{\kappa_k/2} (a_k + a_k^\dagger) F_k - i\sqrt{2\kappa_k} F_k a_k - F_k^2 \right) dt |\psi\rangle \\ & + \left(\sum_j \sqrt{2\kappa_j} \left(a_j + \langle a_j + a_j^\dagger \rangle / 2 \right) - iF_k \right) d\zeta |\psi\rangle. \end{aligned} \quad (\text{C2})$$

Starting from the equation above we now follow the same lines as in Sec. III, i.e. we project the equation onto a Bargmann coherent state $|y\rangle$, define the auxiliary states $|\psi^{(n)}\rangle = (ig\partial_{y^*})^n \langle y|\psi\rangle$ and obtain the HEOM from $\rho_A^{(n,m)} = E_y [[\psi^{(n)}]\langle\psi^{(m)}|]$. This leads us to

$$d\rho_A^{(n,m)} = d_{msmt.} \rho_A^{(n,m)} + d_{fb} \rho_A^{(n,m)}, \quad (\text{C3})$$

where $d_{msmt.} \rho_A^{(n,m)}$ is given as the left hand side of Eq. (17) and describes the change of the state due to the continuously measured evolution. The new terms introduced through the feedback are captured by $d_{fb} \rho_A^{(n,m)}$, which is given in Eq. (24).

[1] H. M. Wiseman and G. J. Milburn, *Quantum Measurement and Control* (Cambridge University Press, 2009).

[2] A. Barchielli and V. P. Belavkin, Measurements continuous in time and a posteriori states in quantum mechanics, *Journal of Physics A: Mathematical and General* **24**, 1495 (1991).

[3] H. M. Wiseman and G. J. Milburn, Interpretation of quantum jump and diffusion processes illustrated on the Bloch sphere, *Phys. Rev. A* **47**, 1652 (1993).

[4] J. Dalibard, Y. Castin, and K. Mølmer, Wave-function approach to dissipative processes in quantum optics, *Phys. Rev. Lett.* **68**, 580 (1992).

[5] K. Mølmer, Y. Castin, and J. Dalibard, Monte Carlo wave-function method in quantum optics, *J. Opt. Soc. Am. B* **10**, 524 (1993).

[6] C. W. Gardiner, A. S. Parkins, and P. Zoller, Wave-function quantum stochastic differential equations and quantum-jump simulation methods, *Phys. Rev. A* **46**, 4363 (1992).

[7] N. Gisin and I. C. Percival, The quantum-state diffusion model applied to open systems, *Journal of Physics A: Mathematical and General* **25**, 5677 (1992).

[8] H. J. Carmichael, *An Open Systems Approach to Quantum Optics* (Springer, Berlin, Germany, 1993).

[9] M. B. Plenio and P. L. Knight, The quantum-jump approach to dissipative dynamics in quantum optics, *Rev. Mod. Phys.* **70**, 101 (1998).

[10] K. Jacobs, *Quantum Measurement Theory and its Applications* (Cambridge University Press, 2014).

[11] A. J. Daley, Quantum trajectories and open many-body quantum systems, *Adv. Phys.* **63**, 77 (2014).

[12] J. Zhang, Y.-x. Liu, R.-B. Wu, K. Jacobs, and F. Nori, Quantum feedback: Theory, experiments, and applications, *Phys. Rep.* **679**, 1 (2017).

[13] L. K. Thomsen, S. Mancini, and H. M. Wiseman, Spin squeezing via quantum feedback, *Phys. Rev. A* **65**,

061801 (2002).

[14] C. Sayrin, I. Dotsenko, X. Zhou, B. Peaudecerf, T. Rybarczyk, S. Gleyzes, P. Rouchon, M. Mirrahimi, H. Amini, M. Brune, J.-M. Raimond, and S. Haroche, Real-time quantum feedback prepares and stabilizes photon number states, *Nature* **477**, 73 (2011).

[15] D. Vitali, P. Tombesi, and G. J. Milburn, Controlling the Decoherence of a "Meter" via Stroboscopic Feedback, *Phys. Rev. Lett.* **79**, 2442 (1997).

[16] J. Wang, H. M. Wiseman, and G. J. Milburn, Dynamical creation of entanglement by homodyne-mediated feedback, *Phys. Rev. A* **71**, 042309 (2005).

[17] J.-G. Li, J. Zou, B. Shao, and J.-F. Cai, Steady atomic entanglement with different quantum feedbacks, *Phys. Rev. A* **77**, 012339 (2008).

[18] S. Gopalakrishnan, B. L. Lev, and P. M. Goldbart, Emergent crystallinity and frustration with Bose-Einstein condensates in multimode cavities, *Nature Physics* **5**, 845 (2009).

[19] S. Gopalakrishnan, B. L. Lev, and P. M. Goldbart, Atom-light crystallization of Bose-Einstein condensates in multimode cavities: Nonequilibrium classical and quantum phase transitions, emergent lattices, supersolidity, and frustration, *Phys. Rev. A* **82**, 043612 (2010).

[20] S. Gopalakrishnan, B. L. Lev, and P. M. Goldbart, Frustration and Glassiness in Spin Models with Cavity-Mediated Interactions, *Phys. Rev. Lett.* **107**, 277201 (2011).

[21] A. T. Black, H. W. Chan, and V. Vuletić, Observation of Collective Friction Forces due to Spatial Self-Organization of Atoms: From Rayleigh to Bragg Scattering, *Phys. Rev. Lett.* **91**, 203001 (2003).

[22] H. Ritsch, P. Domokos, F. Brennecke, and T. Esslinger, Cold atoms in cavity-generated dynamical optical potentials, *Rev. Mod. Phys.* **85**, 553 (2013).

[23] A. J. Kollár, A. T. Papageorge, K. Baumann, M. A. Armen, and B. L. Lev, An adjustable-length cavity and Bose-Einstein condensate apparatus for multimode cavity QED, *New Journal of Physics* **17**, 043012 (2015).

[24] A. J. Kollár, A. T. Papageorge, V. D. Vaidya, Y. Guo, J. Keeling, and B. L. Lev, Supermode-density-wave-polariton condensation with a Bose-Einstein condensate in a multimode cavity, *Nat. Commun.* **8**, 1 (2017).

[25] V. D. Vaidya, Y. Guo, R. M. Kroeze, K. E. Ballantine, A. J. Kollár, J. Keeling, and B. L. Lev, Tunable-Range, Photon-Mediated Atomic Interactions in Multimode Cavity QED, *Phys. Rev. X* **8**, 011002 (2018).

[26] F. Mivehvar, F. Piazza, T. Donner, and H. Ritsch, Cavity QED with quantum gases: new paradigms in many-body physics, *Advances in Physics* **70**, 1 (2021).

[27] A. Wickenbrock, M. Hemmerling, G. R. M. Robb, C. Emery, and F. Renzoni, Collective strong coupling in multimode cavity QED, *Phys. Rev. A* **87**, 043817 (2013).

[28] B. P. Marsh, Y. Guo, R. M. Kroeze, S. Gopalakrishnan, S. Ganguli, J. Keeling, and B. L. Lev, Enhancing Associative Memory Recall and Storage Capacity Using Confocal Cavity QED, *Phys. Rev. X* **11**, 021048 (2021).

[29] V. Torggler, P. Aumann, H. Ritsch, and W. Lechner, A Quantum N-Queens Solver, *Quantum* **3**, 149 (2019).

[30] K. Baumann, C. Guerlin, F. Brennecke, and T. Esslinger, Dicke quantum phase transition with a superfluid gas in an optical cavity, *Nature* **464**, 1301 (2010).

[31] F. Ferri, R. Rosa-Medina, F. Finger, N. Dogra, M. Soriente, O. Zilberberg, T. Donner, and T. Esslinger, Emerging Dissipative Phases in a Superradiant Quantum Gas with Tunable Decay, *Phys. Rev. X* **11**, 041046 (2021).

[32] S. J. Masson and S. Parkins, Rapid Production of Many-Body Entanglement in Spin-1 Atoms via Cavity Output Photon Counting, *Phys. Rev. Lett.* **122**, 103601 (2019).

[33] S. Schmidt and J. Koch, Circuit QED lattices: Towards quantum simulation with superconducting circuits, *Ann. Phys.* **525**, 395 (2013).

[34] C. Noh and D. G. Angelakis, Quantum simulations and many-body physics with light, *Reports on Progress in Physics* **80**, 016401 (2016).

[35] A. Blais, A. L. Grimsmo, S. M. Girvin, and A. Wallraff, Circuit quantum electrodynamics, *Rev. Mod. Phys.* **93**, 025005 (2021).

[36] S. Flannigan, F. Damanet, and A. J. Daley, Many-body quantum state diffusion for non-Markovian dynamics in strongly interacting systems, *arXiv* (2021).

[37] R. G. Lena and A. J. Daley, Dissipative dynamics and cooling rates of trapped impurity atoms immersed in a reservoir gas, *Phys. Rev. A* **101**, 033612 (2020).

[38] I. de Vega, D. Porras, and J. I. Cirac, Matter-Wave Emission in Optical Lattices: Single Particle and Collective Effects, *Phys. Rev. Lett.* **101**, 260404 (2008).

[39] C. Navarrete-Benlloch, I. de Vega, D. Porras, and J. I. Cirac, Simulating quantum-optical phenomena with cold atoms in optical lattices, *New Journal of Physics* **13**, 023024 (2011).

[40] K. Santhosh, O. Bitton, L. Chuntonov, and G. Haran, Vacuum Rabi splitting in a plasmonic cavity at the single quantum emitter limit, *Nature Communications* **7**, ncomms11823 (2016).

[41] S. Franke, S. Hughes, M. K. Dezfouli, P. T. Kristensen, K. Busch, A. Knorr, and M. Richter, Quantization of Quasinormal Modes for Open Cavities and Plasmonic Cavity Quantum Electrodynamics, *Phys. Rev. Lett.* **122**, 213901 (2019).

[42] N. Megier, W. T. Strunz, and K. Luoma, Continuous quantum measurement for general Gaussian unravelings can exist, *Phys. Rev. Research* **2**, 043376 (2020).

[43] A. Imamoglu, Stochastic wave-function approach to non-Markovian systems, *Phys. Rev. A* **50**, 3650 (1994).

[44] B. J. Dalton, S. M. Barnett, and B. M. Garraway, Theory of pseudomodes in quantum optical processes, *Phys. Rev. A* **64**, 053813 (2001).

[45] B. M. Garraway, Nonperturbative decay of an atomic system in a cavity, *Phys. Rev. A* **55**, 2290 (1997).

[46] G. Pleasance, B. M. Garraway, and F. Petruccione, Generalized theory of pseudomodes for exact descriptions of non-Markovian quantum processes, *Phys. Rev. Research* **2**, 043058 (2020).

[47] L. Mazzola, S. Maniscalco, J. Piilo, K.-A. Suominen, and B. M. Garraway, Pseudomodes as an effective description of memory: Non-Markovian dynamics of two-state systems in structured reservoirs, *Phys. Rev. A* **80**, 012104 (2009).

[48] H. Yang, H. Miao, and Y. Chen, Nonadiabatic elimination of auxiliary modes in continuous quantum measurements, *Phys. Rev. A* **85**, 040101 (2012).

[49] H.-P. Breuer, Genuine quantum trajectories for non-Markovian processes, *Phys. Rev. A* **70**, 012106 (2004).

[50] A. Barchielli, C. Pellegrini, and F. Petruccione, Stochastic Schrödinger equations with coloured noise, *EPL (Europhysics Letters)* **91**, 24001 (2010).

[51] Y. Tanimura, Numerically “exact” approach to open quantum dynamics: The hierarchical equations of motion (HEOM), *The Journal of Chemical Physics* **153**, 020901 (2020).

[52] K. Nakamura and Y. Tanimura, Hierarchical Schrödinger equations of motion for open quantum dynamics, *Phys. Rev. A* **98**, 012109 (2018).

[53] Y. Guo, R. M. Kroese, V. D. Vaidya, J. Keeling, and B. L. Lev, Sign-Changing Photon-Mediated Atom Interactions in Multimode Cavity Quantum Electrodynamics, *Phys. Rev. Lett.* **122**, 193601 (2019).

[54] Y. Guo, V. D. Vaidya, R. M. Kroese, R. A. Lunney, B. L. Lev, and J. Keeling, Emergent and broken symmetries of atomic self-organization arising from Gouy phase shifts in multimode cavity QED, *Phys. Rev. A* **99**, 053818 (2019).

[55] E. T. Jaynes and F. W. Cummings, Comparison of quantum and semiclassical radiation theories with application to the beam maser, *Proceedings of the IEEE* **51**, 89 (1963).

[56] V. Gorini, A. Kossakowski, and E. C. G. Sudarshan, Completely positive dynamical semigroups of N-level systems, *J. Math. Phys.* **17**, 821 (1976).

[57] G. Lindblad, On the generators of quantum dynamical semigroups, *Commun. Math. Phys.* **48**, 119 (1976).

[58] R. Palacino and J. Keeling, Atom-only theories for u(1) symmetric cavity-qed models, *Phys. Rev. Research* **3**, L032016 (2021).

[59] F. Damanet, A. J. Daley, and J. Keeling, Atom-only descriptions of the driven-dissipative Dicke model, *Phys. Rev. A* **99**, 033845 (2019).

[60] Y. Tanimura, Stochastic Liouville, Langevin, Fokker-Planck, and Master Equation Approaches to Quantum Dissipative Systems, *Journal of the Physical Society of Japan* **75**, 082001 (2006).

[61] Y. Tanimura, Reduced hierarchical equations of motion in real and imaginary time: Correlated initial states and thermodynamic quantities, *The Journal of Chemical Physics* **141**, 044114 (2014).

[62] Y. Tanimura and R. Kubo, Two-Time Correlation Functions of a System Coupled to a Heat Bath with a Gaussian-Markoffian Interaction, *Journal of the Physical Society of Japan* **58**, 1199 (1989).

[63] L. Diósi and W. T. Strunz, The non-Markovian stochastic Schrödinger equation for open systems, *Physics Letters A* **235**, 569 (1997).

[64] L. Diósi, N. Gisin, and W. T. Strunz, Non-Markovian quantum state diffusion, *Phys. Rev. A* **58**, 1699 (1998).

[65] W. T. Strunz, L. Diósi, and N. Gisin, Open system dynamics with non-Markovian quantum trajectories, *Phys. Rev. Lett.* **82**, 1801 (1999).

[66] A. Shabani, J. Roden, and K. B. Whaley, Continuous Measurement of a Non-Markovian Open Quantum System, *Phys. Rev. Lett.* **112**, 113601 (2014).

[67] W. Jiang, F.-Z. Wu, and G.-J. Yang, Non-Markovian entanglement dynamics of open quantum systems with continuous measurement feedback, *Phys. Rev. A* **98**, 052134 (2018).

[68] D. Walls and G. Milburn, *Quantum Optics* (Springer Berlin Heidelberg, 2008).

[69] J. Gambetta and H. M. Wiseman, Non-Markovian stochastic Schrödinger equations: Generalization to real-valued noise using quantum-measurement theory, *Phys. Rev. A* **66**, 012108 (2002).

[70] J. Piilo, S. Maniscalco, K. Härkönen, and K.-A. Suominen, Non-Markovian Quantum Jumps, *Phys. Rev. Lett.* **100**, 180402 (2008).

[71] K. Luoma, W. T. Strunz, and J. Piilo, Diffusive Limit of Non-Markovian Quantum Jumps, *Phys. Rev. Lett.* **125**, 150403 (2020).

[72] L. Diósi, Non-Markovian Continuous Quantum Measurement of Retarded Observables, *Phys. Rev. Lett.* **100**, 080401 (2008).

[73] L. Diósi, Erratum: Non-Markovian Continuous Quantum Measurement of Retarded Observables [Phys. Rev. Lett. 100, 080401 (2008)], *Phys. Rev. Lett.* **101**, 149902 (2008).

[74] M. W. Jack and M. J. Collett, Continuous measurement and non-Markovian quantum trajectories, *Phys. Rev. A* **61**, 062106 (2000).

[75] H. M. Wiseman and J. M. Gambetta, Pure-State Quantum Trajectories for General Non-Markovian Systems Do Not Exist, *Phys. Rev. Lett.* **101**, 140401 (2008).

[76] J. Gambetta and H. M. Wiseman, Interpretation of non-Markovian stochastic Schrödinger equations as a hidden-variable theory, *Phys. Rev. A* **68**, 062104 (2003).

[77] S. Krönke and W. T. Strunz, Non-Markovian quantum trajectories, instruments and time-continuous measurements, *Journal of Physics A: Mathematical and Theoretical* **45**, 055305 (2012).

[78] D. Suess, A. Eisfeld, and W. T. Strunz, Hierarchy of Stochastic Pure States for Open Quantum System Dynamics, *Phys. Rev. Lett.* **113**, 150403 (2014).

[79] R. Hartmann and W. T. Strunz, Exact Open Quantum System Dynamics Using the Hierarchy of Pure States (HOPS), *Journal of Chemical Theory and Computation* **13**, 5834 (2017), pMID: 29016126.

[80] D. Suess, W. T. Strunz, and A. Eisfeld, Hierarchical Equations for Open System Dynamics in Fermionic and Bosonic Environments, *J. Stat. Phys.* **159**, 1408 (2015).

[81] Z. Tang, X. Ouyang, Z. Gong, H. Wang, and J. Wu, Extended hierarchy equation of motion for the spin-boson model, *The Journal of Chemical Physics* **143**, 224112 (2015).

[82] F. Dimer, B. Estienne, A. S. Parkins, and H. J. Carmichael, Proposed realization of the Dicke-model quantum phase transition in an optical cavity QED system, *Phys. Rev. A* **75**, 013804 (2007).

[83] H. J. Groenewold, A problem of information gain by quantal measurements, *International Journal of Theoretical Physics* **4**, 327 (1971).

[84] G. Vidal and R. F. Werner, Computable measure of entanglement, *Phys. Rev. A* **65**, 032314 (2002).

[85] P.-P. Zhang, C. D. B. Bentley, and A. Eisfeld, Flexible scheme to truncate the hierarchy of pure states, *J. Chem. Phys.* **148**, 134103 (2018).

[86] P. Warszawski and H. M. Wiseman, Adiabatic elimination in compound quantum systems with feedback, *Phys. Rev. A* **63**, 013803 (2000).

[87] L. K. Thomsen, S. Mancini, and H. M. Wiseman, Continuous quantum nondemolition feedback and unconditional atomic spin, *J. Phys. B: At. Mol. Opt. Phys.* **35**, 4937 (2002).

[88] A. Sørensen, L.-M. Duan, J. I. Cirac, and P. Zoller, Many-particle entanglement with Bose-Einstein condensates, *Nature* **409**, 63 (2001).

[89] X. Wang, Spin squeezing in nonlinear spin-coherent states, *J. Opt. B: Quantum Semiclassical Opt.* **3**, 93 (2001).

[90] X. Gao, J. Ren, A. Eisfeld, and Z. Shuai, Non-Markovian Stochastic Schrödinger Equation: Matrix Product State Approach to the Hierarchy of Pure States, *arXiv* (2021).

[91] A. V. Bezvershenko, C.-M. Halati, A. Sheikhan, C. Kollath, and A. Rosch, Dicke Transition in Open Many-Body Systems Determined by Fluctuation Effects, *Phys. Rev. Lett.* **127**, 173606 (2021).

[92] M. Buchhold, Y. Minoguchi, A. Altland, and S. Diehl, Effective Theory for the Measurement-Induced Phase Transition of Dirac Fermions, *Phys. Rev. X* **11**, 041004 (2021).

[93] T. Müller, S. Diehl, and M. Buchhold, Measurement-induced dark state phase transitions in long-ranged fermion systems, *arXiv* (2021).

[94] E. Fiorelli, M. Marcuzzi, P. Rotondo, F. Carollo, and I. Lesanovsky, Signatures of associative memory behavior in a multimode dicke model, *Phys. Rev. Lett.* **125**, 070604 (2020).

[95] S. Schütz, J. Schachenmayer, D. Hagenmüller, G. K. Brennen, T. Volz, V. Sandoghdar, T. W. Ebbesen, C. Genes, and G. Pupillo, Ensemble-Induced Strong Light-Matter Coupling of a Single Quantum Emitter, *Phys. Rev. Lett.* **124**, 113602 (2020).

[96] D. Hagenmüller, S. Schütz, J. Schachenmayer, C. Genes, and G. Pupillo, Cavity-assisted mesoscopic transport of fermions: Coherent and dissipative dynam-ics, *Phys. Rev. B* **97**, 205303 (2018).

[97] J. Schachenmayer, C. Genes, E. Tignone, and G. Pupillo, Cavity-Enhanced Transport of Excitons, *Phys. Rev. Lett.* **114**, 196403 (2015).

[98] D. Hagenmüller, J. Schachenmayer, S. Schütz, C. Genes, and G. Pupillo, Cavity-Enhanced Transport of Charge, *Phys. Rev. Lett.* **119**, 223601 (2017).

[99] C. Maier, T. Brydges, P. Jurcevic, N. Trautmann, C. Hempel, B. P. Lanyon, P. Hauke, R. Blatt, and C. F. Roos, Environment-Assisted Quantum Transport in a 10-qubit Network, *Phys. Rev. Lett.* **122**, 050501 (2019).

[100] J. B. Curtis, Z. M. Raines, A. A. Allocsa, M. Hafezi, and V. M. Galitski, Cavity Quantum Eliashberg Enhancement of Superconductivity, *Phys. Rev. Lett.* **122**, 167002 (2019).

[101] S. Uchino, M. Ueda, and J.-P. Brantut, Universal noise in continuous transport measurements of interacting fermions, *Phys. Rev. A* **98**, 063619 (2018).

[102] V. Vuletić, H. W. Chan, and A. T. Black, Three-dimensional cavity Doppler cooling and cavity sideband cooling by coherent scattering, *Phys. Rev. A* **64**, 033405 (2001).

[103] J. Zeiher, J. Wolf, J. A. Isaacs, J. Kohler, and D. M. Stamper-Kurn, Tracking Evaporative Cooling of a Mesoscopic Atomic Quantum Gas in Real Time, *Phys. Rev. X* **11**, 041017 (2021).

[104] F. O. Prado, F. S. Luiz, J. M. Villas-Bôas, A. M. Alcalde, E. I. Duzzioni, and L. Sanz, Atom-mediated effective interactions between modes of a bimodal cavity, *Phys. Rev. A* **84**, 053839 (2011).

[105] Y.-L. Dong, X.-B. Zou, S.-L. Zhang, S. Yang, C.-F. Li, and G.-C. Guo, Cavity-QED-based phase gate for photonic qubits, *Journal of Modern Optics* **56**, 1230 (2009).